Analysis of Two Polyhydroxyalkanoate Synthases in *Bradyrhizobium japonicum* USDA 110

J. Ignacio Quelas,[a] Elías J. Mongiardini,[a] Julieta Pérez-Giménez,[a] Gustavo Parisi,[b] Aníbal R. Lodeiro[a]

Instituto de Biotecnología y Biología Molecular (IBBM), Departamento de Ciencias Biológicas, Facultad de Ciencias Exactas, Universidad Nacional de La Plata, and CCT La Plata-CONICET, La Plata, Argentina[a]; Unidad de Bioinformática Estructural, Departamento de Ciencia y Tecnología, Universidad Nacional de Quilmes, Bernal, Argentina[b]

Bradyrhizobium japonicum USDA 110 has five polyhydroxyalkanoate (PHA) synthases (PhaC) annotated in its genome: *bll4360* (*phaC1*), *bll6073* (*phaC2*), *blr3732* (*phaC3*), *blr2885* (*phaC4*), and *bll4548* (*phaC5*). All these proteins possess the catalytic triad and conserved amino acid residues of polyester synthases and are distributed into four different PhaC classes. We obtained mutants in each of these paralogs and analyzed *phaC* gene expression and PHA production in liquid cultures. Despite the genetic redundancy, only *phaC1* and *phaC2* were expressed at significant rates, while PHA accumulation in stationary-phase cultures was impaired only in the ΔphaC1 mutant. Meanwhile, the ΔphaC2 mutant produced more PHA than the wild type under this condition, and surprisingly, the *phaC3* transcript increased in the ΔphaC2 background. A double mutant, the ΔphaC2 ΔphaC3 mutant, consistently accumulated less PHA than the ΔphaC2 mutant. PHA accumulation in nodule bacteroids followed a pattern similar to that seen in liquid cultures, being prevented in the ΔphaC1 mutant and increased in the ΔphaC2 mutant in relation to the level in the wild type. Therefore, we used these mutants, together with a ΔphaC1 ΔphaC2 double mutant, to study the *B. japonicum* PHA requirements for survival, competition for nodulation, and plant growth promotion. All mutants, as well as the wild type, survived for 60 days in a carbon-free medium, regardless of their initial PHA contents. When competing for nodulation against the wild type in a 1:1 proportion, the ΔphaC1 and ΔphaC1 ΔphaC2 mutants occupied only 13 to 15% of the nodules, while the ΔphaC2 mutant occupied 81%, suggesting that the PHA polymer is required for successful competitiveness. However, the bacteroid content of PHA did not affect the shoot dry weight accumulation.

Rhizobia are soil bacteria that may live in two states: as free-living bacteria in the soil or as symbiotic bacteroids inside legume nodules. Soybean plants form determinate nodules, which are round and maintain the oldest infected cells at their center (1, 2). Bacteroids inside these determinate nodules synthesize polyhydroxyalkanoates (PHAs), which may serve as carbon- and energy-reserve polymers that are stored in complex cytoplasmic granules. In addition, bacteroids from determinate nodules are able to dedifferentiate back to free-living rhizobia once the nodule senesces (3).

PHA is of great interest due to its potential use as a biodegradable plastic (4). The cellular functions of PHA are related to the cell's metabolic balance, and PHA is especially useful to the cell as an energy and reductant reserve (5). In rhizobia, where PHA contributes to reproduction and survival (6), this polymer is synthesized in three steps (see Fig. S1 in the supplemental material): the condensation of two acetyl coenzyme A (acetyl-CoA) molecules to synthesize acetoacetyl-CoA is catalyzed by β-ketothiolase (PhaA), the reduction of acetoacetyl-CoA to hydroxyacyl-CoA in an NADPH-dependent reaction is catalyzed by NADP–acetoacetyl-CoA reductase (PhaB), and the polymerization of hydroxyacyl-CoA into PHA is catalyzed by PHA synthase (PhaC). The last enzyme is essential for PHA synthesis in all rhizobial species (5).

Although most sequenced rhizobia have one or two *phaC* homologs in their genomes, five putative *phaC* open reading frames (ORFs) have been detected in *Bradyrhizobium japonicum* USDA 110 (7) and are named *bll4360*, *bll6073*, *blr3732*, *blr2885*, and *bll4548* (henceforth *phaC1*, *phaC2*, *phaC3*, *phaC4*, and *phaC5*, respectively). However, experimental evidence about the expression of these genes is available only for *phaC1* and *phaC2*. In a proteomic study of soybean nodule bacteroids, Sarma and Emerich

(8) detected PhaC2. This observation is consistent with that from another, transcriptomic study, in which the *phaC2* transcript was observed to be significantly expressed in nodules and in microaerobiosis (9), as well as with the observation that *phaC2* expression is promoted by FixK$_2$, which is a transcription factor that is regulated by O$_2$ levels (10, 11). Pessi and coworkers (9) also observed that in contrast to *phaC2*, *phaC1* is downregulated in bacteroids in comparison to its regulation in aerobic free-living bacteria. In agreement with the last observation, Franck and coworkers (12) reported that *phaC1* is upregulated in free-living chemoautotrophic bacteria, while *phaC2* is downregulated in the same state. However, more recent proteomic and transcriptomic studies have indicated that both *phaC1* and *phaC2* are present in nodule bacteroids (13, 14). In a different study, Aneja and coworkers attempted to complement a *phaC*-defective *Ensifer* (formerly *Sinorhizobium*) *meliloti* mutant with a *B. japonicum* cosmid library in order to isolate genes encoding functional PHA synthases in this rhizobial species and were successful only with *phaC1* (15).

These studies suggest that *phaC1* and *phaC2* might be specifically required in the free-living and bacteroid states, respectively. However, this suggestion is based only on expression studies, since PhaC1

TABLE 1 Plasmids and bacterial strains used in this study

Plasmid or strain	Relevant characteristics	Reference or source
Plasmids		
pRK2013	ColE1 replicon, Tra$^+$ from RK2, Km^r	52
pGEM-T Easy	Multicopy vector, Ap^r	Promega
pK18mob	Mob$^+$ Km^r, suicide vector in rhizobia	53
pG18mob2	Mob$^+$ Gm^r, suicide vector in rhizobia	54
pBBR1MCS2-5	Km^r Gm^r, broad-host-range vector	55
pHP45Ω	Ap^r Sm^r Sp^r, donor of Ω-Sm-Sp interposon	56
pUC4K	Ap^r Km^r, donor of *nptI* cassette	57
pFAJ1708	Ap^r Tc^r, *nptII* constitutive promoter and RK2 *par* locus, replicative in Gram-negative bacteria	21
pIQ16	Derived from pGEM-T Easy with fragment 1 (310 bp), amplified with Fw1 and Rv1 (C terminus of *bll4360* spanning bases 4821923 to 4821613)	This work
pIQ17	Derived from pGEM-T Easy with fragment 2 (383 bp), amplified with Fw2 and Rv2 (N terminus of *bll4360* spanning bases 4820220 to 4820603)	This work
pIQ18	Derived from pGEM-T Easy with fragment 3 (379 bp), amplified with Fw3 and Rv3 (C terminus of *bll6073* spanning bases 6689165 to 6689544)	This work
pIQ19	Derived from pGEM-T Easy with fragment 4 (330 bp), amplified with Fw4 and Rv4 (N terminus of *bll6073* spanning bases 6691078 to 6691408)	This work
pIQ20	Derived from pBBR1MCS5 plus fragment 1 (328-bp EcoRI-digested fragment from pIQ16)	This work
pIQ21	Derived from pBBR1MCS5 plus fragment 3 (397-bp EcoRI-digested fragment from pIQ18)	This work
pIQ22	Derived from pK18mob plus fragment 2 (445-bp SphI-PstI-digested fragment from pIQ17)	This work
pIQ23	Derived from pG18mob2 plus fragment 4 (348-bp EcoRI-digested fragment from pIQ19)	This work
pIQ24	Derived from pIQ22, plus fragment 1 (402-bp XbaI-KpnI-digested fragment from pIQ20)	This work
pIQ25	Derived from pIQ23 plus fragment 3 (411-bp HindIII-PstI-digested fragment from pIQ20)	This work
pIQ26	Derived from pIQ24 plus Ω-Sm-Sp interposon from SmaI-digested pHP45	This work
pIQ27	Derived from pIQ25 plus *nptI* cassette from SalI-digested pUC4K	This work
pIQ28	Derived from pBBR1MCS2 plus 2,110 bp amplified with Fw5 and Rv5 carrying the entire *bll4360* ORF (bases 4822091 to 4819981) cloned into SmaI	This work
pIQ29	Derived from pBBR1MCS2 plus 2,379 bp amplified with Fw6 and Rv6 carrying the entire *bll6073* ORF (bases 6691245 to 6688866) cloned into SmaI	This work
pIQ30	Derived from pFAJ1708 plus 2,180 bp from BamHI-KpnI-digested pIQ28 controlled by *nptII* promoter	This work
pIQ31	Derived from pFAJ1708 plus 2,479 bp from XbaI-KpnI-digested pIQ29 controlled by *nptII* promoter	This work
pIQ32	Derived from pG18mob2 with 312 bp (bases 4141805 to 4142117) of *blr3732* internal fragment amplified with Fw5 and Rv5 cloned into SmaI	This work
pIQ33	Derived from pG18mob2 with 212 bp (bases 3179424 to 3179636) of *blr2885* internal fragment amplified with Fw6 and Rv6 cloned into SmaI	This work
pIQ34	Derived from pG18mob2 with 230 bp (bases 5041752 to 5041982) of *blr4548* internal fragment amplified with Fw7 and Rv7 cloned into SmaI	This work
Strains		
USDA 110	*Bradyrhizobium japonicum* wild type, Cm^r	USDA culture collection
LP 2885	*B. japonicum* with pG18mob2 inserted at base 3179636 of *bll2885*, Gm^r derivative of USDA 110	This work
LP 3732	*B. japonicum* with pG18mob2 inserted at base 4142117 of *bll3732*, Gm^r derivative of USDA 110	This work
LP 4360	*B. japonicum* with Ω-Sm-Sp replacing central 1,031 bp of *bll4360*, Sm^r Sp^r derivative of USDA 110	This work
LP 4548	*B. japonicum* with pG18mob2 inserted at base 5041982 of *bll4548*, Gm^r derivative of USDA 110	This work
LP 6073	*B. japonicum* with *nptI* cassette replacing central 1,267 bp of *bll6073*, Km^r derivative of USDA 110	This work
LP 6060	*B. japonicum* with *nptI* cassette replacing central 1,267 bp of *bll6073*, Sm^r Sp^r Km^r derivative of LP 4360	This work
LP 7337	*B. japonicum* with pG18mob2 inserted at base 4142117 of *bll3732*, Gm^r Km^r derivative of LP 6073	This work
DH5α	*Escherichia coli recA lacU169* φ80d*lacZ*ΔM15	Bethesda Research Laboratories
S17-1	*E. coli thi proA hsdR17 hasdM$^+$ recA* RP4-Tra function	58

is the only paralog for which proof of biological activity is available (15). In addition, there are no data on the possible functionality of the other three putative *phaC* paralogs mentioned above. To get a better understanding of the possible role of these different PHA synthases in the survival of the free-living state and the symbiotic efficiency of this species, we studied their requirement for PHA production, as well as the impact of this reserve polymer on growth kinetics, survival, competitiveness for nodulation, and plant growth-promoting activity.

MATERIALS AND METHODS

Bacterial strains and culture conditions. Strains and plasmids are summarized in Table 1. *B. japonicum* was grown in Götz minimal medium with mannitol as the sole carbon source (16). The total biomass was estimated by measurement of the optical density at 500 nm (OD$_{500}$) and the number of viable bacteria on the basis of the number of CFU on yeast extract-mannitol (17) agar (YMA) plates. For conjugation, peptone salts-yeast extract (PSY) medium (18) was employed. *Escherichia coli* was

grown in Luria-Bertani (LB) medium ([19]). Antibiotics were added to the media at the following concentrations (μg ml^{-1}): streptomycin (Sm), 400 (*B. japonicum*) or 100 (*E. coli*); spectinomycin (Sp), 200 (*B. japonicum*) or 100 (*E. coli*); kanamycin (Km), 150 (*B. japonicum*) or 25 (*E. coli*); ampicillin (Ap), 200 (*E. coli*); gentamicin (Gm), 100 (*B. japonicum*) or 10 (*E. coli*); tetracycline (Tc) 20 and 50 (*B. japonicum* liquid and solid cultures, respectively) or 10 (*E. coli*); and chloramphenicol (Cm), 20 (*B. japonicum*).

Genetic techniques and DNA manipulation. Cloning procedures, including DNA isolation, restriction digestion, ligation, and transformation, were performed as described previously ([19]). Tri- or biparental matings were performed with the *E. coli* DH5α or S17-1 strain, as has been previously described ([20]). Electroporation was performed with a Gene Pulser system (Bio-Rad, Hercules, CA) at 1.5 V, 25 μF, and 200 Ω in a 0.1-cm-gap-width electroporation cuvette.

Oligonucleotide primers were purchased from Life Technologies (Buenos Aires, Argentina). DNA amplification was performed by PCR using *Taq* DNA polymerase (Life Technologies, Buenos Aires, Argentina) for routine PCR or KAPA HiFi hot-start (HS) DNA polymerase (Kapabiosystems, Woburn, MA) for the amplification of targets longer than 1,000 bp in a Bioer Life Express thermocycler (Hangzhou, China). DNA sequencing was performed at Macrogen Corp. (Seoul, South Korea).

To construct the *B. japonicum phaC* mutants, primers specific for *bll4360* (*phaC1*), *bll6073* (*phaC2*), *blr3732* (*phaC3*), *blr2885* (*phaC4*), and *bll4548* (*phaC5*) were designed (see Table S1 in the supplemental material). For *phaC1* and *phaC2*, fragments of *B. japonicum* USDA 110 genomic DNA were generated from both sides of the target coding sequences. For *phaC1*, an upstream fragment of 310 bp and a downstream fragment of 383 bp were amplified using primers Fw1/Rv1 (fragment 1) and Fw2/Rv2 (fragment 2), respectively. These PCR fragments were cloned into pGEM-T Easy separately, creating pIQ16 and pIQ17, respectively. pIQ16 was then digested with EcoRI and subcloned into pBBR1MCS5, creating pIQ20. pIQ17 was digested with SphI and PstI and subcloned into pK18mob, creating pIQ22. The pIQ22 plasmid was digested with XbaI and KpnI, and the 402-bp XbaI-KpnI-digested fragment 1 product from pIQ20 was cloned at this site, generating pIQ24. The pIQ24 vector was subsequently digested with SmaI (resulting in a cut between fragments 1 and 2) and ligated with the SmaI-digested Ω-Sm-Sp interposon from pHP45, generating pIQ26. Gene replacement was performed by introducing pIQ26 into the wild-type strain *B. japonicum* USDA 110 by biparental mating, selecting by growth on Sm-Sp-supplemented YMA, and screening for Km sensitivity in order to select for the double-crossover event. The resulting strain was designated LP 4360 (ΔphaC1); this strain carries the Ω-Sm-Sp-interposon in place of the genomic DNA from base 4820583 to base 4821613, thus removing 1,031 bp from the center of the 1,803-bp ORF *bll4360* ([7]).

For *phaC2*, an upstream fragment of 379 bp and a downstream fragment of 330 bp were amplified using primers Fw3/Rv3 (fragment 3) and Fw4/Rv4 (fragment 4), respectively. These PCR fragments were cloned into pGEM-T Easy separately, creating pIQ18 and pIQ19, respectively. pIQ18 was digested with EcoRI and subcloned into pBBR1MCS5, creating pIQ21. The pIQ19 vector was digested with EcoRI and subcloned into pG18mob2, creating pIQ23. The pIQ23 plasmid was then digested with HindIII and PstI, and fragment 3 (411 bp) from pIQ21 was cloned at this site, generating pIQ25. The pIQ25 vector was subsequently digested with SalI (resulting in a cut between fragments 3 and 4) and ligated with the SalI-digested *nptI* cassette from pUC4-K, generating pIQ27. Gene replacement was performed by introducing pIQ27 into the wild-type strain *B. japonicum* USDA 110 by triparental mating using the pRK2013 helper plasmid, selecting by growth on Km-supplemented YMA, and screening for Gm sensitivity in order to select for the double-crossover event. Strain LP 6073 (ΔphaC2) carries the *nptI* cassette between bases 6689567 and 6690793 of the genomic DNA, thus replacing 1,226 bp of the 1,842-bp ORF *bll6073*.

The double mutant LP 6060 (ΔphaC1 ΔphaC2) was constructed as described above, introducing pIQ27 in the background of LP 4360.

To construct *B. japonicum phaC3*, *phaC4*, and *phaC5* gene disruption mutants, blunt-end fragments of 312, 212, and 230 bp were amplified using primers Fw5/Rv5, Fw6/Rv6, and Fw7/Rv7, respectively, with KAPA HiFi HS DNA polymerase (Kapabiosystems, Woburn, MA). These PCR fragments were cloned into the SmaI site of pG18mob2 separately, creating plasmids pIQ32, pIQ33, and pIQ34, respectively. Conjugation was performed by introducing these plasmids into the wild-type strain *B. japonicum* USDA 110 by biparental mating using *E. coli* S17-1 as the donor and selecting by growth on Cm- and Gm-supplemented YMA in order to select for single homologous recombination events. The single mutant strains carrying *phaC* insertions have the catalytic triad interrupted by the plasmid vector and were named LP 3732 (ΔphaC3), LP 2885 (ΔphaC4), and LP 4548 (ΔphaC5). The plasmids were inserted at bases 3179636, 4142117, and 5042196 of the genomic DNA, respectively.

The double mutant LP 7337 (ΔphaC2 ΔphaC3) was constructed as described above, introducing pIQ32 in the background of LP 6073.

All the mutations were confirmed by PCR using external primers (see Table S1 in the supplemental material), as described previously ([20]), and by DNA sequencing.

Complementation experiments were performed by integrating the complete sequences of *phaC1* or *phaC2* (amplified with primers Fw1c/Rv1c and Fw2c/Rv2c, respectively) and their putative native promoters (inferred by the BPROM program) into a replicative vector. Briefly, the 2,110-bp *phaC1* and the 2,379-bp *phaC2* target sequences were amplified from *B. japonicum* USDA 110 chromosomal DNA and cloned into the SmaI site of pBBR1MCS2 to create pIQ28 and pIQ29. Then, pIQ28 was digested with BamHI and KpnI and pIQ29 was digested with XbaI and KpnI. Each fragment was inserted in the replicative broad-host-range vector pFAJ1708, generating plasmids pIQ30 (*phaC1*) and pIQ31 (*phaC2*). Recombinant plasmids were cloned with *phaC* genes under the strong, constitutive *nptII* promoter ([21]). These constructions were confirmed by sequencing. Then, each plasmid harboring the complete *phaC1* or *phaC2* gene was transferred into the desired *B. japonicum* strain by biparental mating.

Bioinformatics and *in silico* characterization of PHA synthases. The multiple-sequence alignment was performed using T-COFFEE software ([22]). The phylogenetic analysis was performed using the maximum likelihood method and the PhyML (version 3.0) program ([23]) with bootstrap analysis (1,000 iterations). The tree was constructed using MEGA (version 5.1) software ([24]). The occurrence of conserved residues in the catalytic triad and the lipase box were checked manually.

To estimate the PhaC three-dimensional structure, fold assignment was performed with the FFAS03 ([25]) and HHpred ([26]) programs and *ab initio* fold prediction was performed with the ITASSER program ([27]). The quality of the models was evaluated with the PROSAII program ([28]).

qRT-PCR. Fifteen milliliters of *B. japonicum* liquid cultures was centrifuged at 13,500 × g for 40 min and washed twice with 1 M NaCl. Then, the cells were disrupted with lysozyme in TE (Tris-EDTA) buffer, pH 8.0 (30 min, 37°C). Total RNA was extracted using the TRIzol reagent (Life Technologies, Buenos Aires, Argentina), following the manufacturer's instructions, and its quantity and quality were determined using a Nano-Drop spectrophotometer (NanoDrop Technologies, Wilmington, DE). Aliquots (0.5 μg) were treated with DNase I (30 min, 37°C), and cDNA was synthesized using random hexamer primers with Moloney murine leukemia virus reverse transcriptase (Life Technologies, Buenos Aires, Argentina), following the manufacturer's instructions. To check the quality of the cDNA preparation, PCRs were performed using primers Fw2/Rv2, Fw4/Rv4, Fw5/Rv5, Fw6/Rv6, and Fw7/Rv7 for *phaC1*, *phaC2*, *phaC3*, *phaC4*, and *phaC5*, respectively (see Table S1 in the supplemental material). The absence of contaminating DNA was demonstrated by the lack of PCR amplification in an RNA sample that was not subjected to reverse transcription (RT). The *sigA* primers were used as a positive control ([29]). Quantitative real-time RT-PCR (qRT-PCR) amplification was

performed with primers Fw2/Rv2, Fw4/Rv4, Fw5-Rv5, Fw6/Rv6, and Fw7/Rv7 (see Table S1 in the supplemental material) in a Line-Gene instrument (Bioer, Hangzhou, China), and the amplicons were analyzed with a Line-Gene K fluorescence quantitative detection system (version 4.0.00 software). The ready-to-use iQ SYBR green Supermix (Bio-Rad, Hercules, CA) was used for all of the reactions, according to the manufacturer's instructions. Standard 10-fold serial dilutions of the cDNA samples were used to calculate the PCR efficiency. Standard curves were generated from the purified amplicons for absolute quantification. Normalized expression values were calculated as the ratio of the absolute quantities of the gene of interest to the absolute quantities of the housekeeping gene *sigA*.

Carbon starvation survival assay. Fifty-milliliter bottles containing 15 ml of Götz medium without a carbon source were inoculated with 19-day-old *B. japonicum* cells. To prepare the inocula, the cultures were pelleted and washed twice with sterile 0.5% NaCl at a final OD_{500} of 0.2. These cell suspensions were maintained at 28°C with shaking at 180 rpm, and the numbers of CFU were periodically counted from 0 to 60 days.

Quantification of PHA. *B. japonicum* cultures were twice centrifuged at $12,000 \times g$ for 40 min. Then, the pellet was homogenized with sodium hypochlorite overnight at room temperature, washed with double-distilled water, precipitated with 1:1 alcohol-acetone, and resuspended in chloroform. Then, PHA was determined as chrotonic acid in H_2SO_4 (30).

To determine the PHA content of bacteroid cells, seven mature nodules (weight, 60 to 90 mg) were crushed and homogenized, suspended in 1 ml of double-distilled water, and centrifuged for 5 min at $5,000 \times g$. The supernatants were then processed for the determination of PHA levels, as has been previously described (16).

Plant experiments. DonMario 3810 soybean seeds, kindly provided by DonMario SA, Argentina, were surface sterilized and germinated as has been previously described (20). Plants were sown in sterile vermiculite pots containing modified N-free Fåhraeus plant nutrient solution (20) and grown for the indicated times in a greenhouse at temperatures of 26°C and 18°C during the day and at night, respectively, with uncontrolled relative humidity, which varied from about 60% during the day to 90% at night. The pots were irrigated with sterile distilled water every 4 days and provided one watering with 1:5-diluted nitrogen-free plant nutrient solution every 15 days.

To study competition for nodulation, we inoculated 10 vermiculite pots containing 3-day-old soybean plantlets with bacterial mixtures of strain USDA 110 and each mutant strain ($\Delta phaC1$, $\Delta phaC2$, or $\Delta phaC1$ $\Delta phaC2$ strain) in a 1:1 proportion, as has been described previously (20). Each mixed inoculum was freshly prepared by dilution of early-stationary-phase liquid cultures (9 days old). As controls, two pots were kept uninoculated and sets of two pots each were inoculated with each competitor strain and unmixed. After 21 days in the greenhouse, nodules were excised, surface sterilized, and crushed, and their contents were grown in YMA plates to obtain the occupying rhizobia, as has been previously described (20). Nodule occupation was evaluated on the basis of the antibiotic resistance of the strains that were recovered from the nodules, after the recovered bacteria were inoculated in replicate YMA plates containing selective antibiotics. The statistical analysis was carried out using the χ^2 method, considering 45% nodule occupation by each strain alone and 10% double occupation to be the null hypothesis (31).

Plant growth parameters were assessed in 67-day-old plants. Shoots or nodules from each plant were cut and dried in an oven at 60°C to a constant weight, and the materials from each plant were weighed individually. The statistical analysis of shoot dry weight, nodule number, and nodule dry weight per plant was performed by a one-way analysis of variance (ANOVA), with significance being a P value of <0.05.

Microscopy. Bacteria from liquid cultures and nodules excised from plants (each one transversally cut in halves) were collected and fixed in 2% (vol/vol) glutaraldehyde, as has been described previously (20). Next, the samples were dehydrated, infiltrated with epoxy resin, sectioned, and stained, as has been described previously (20). Transmission electron mi-

croscopy of the glutaraldehyde-fixed samples was performed as has been described previously (20). The grids were viewed at 80 kV in a JEM1200 EX II transmission electron microscope (JEOL Ltd., Tokyo, Japan), and micrographs were obtained with an ES500W Erlangshen charge-coupled-device camera (Gatan Inc., Pleasanton, CA).

To measure the bacterial major longitudinal cell size in free-living bacteria, pictures of 200 cells of each strain taken as described above were evaluated using ImageJ software (32).

For light microscopy, glutaraldehyde-fixed 2-μm-thick sections of nodules were dried onto glass slides, stained with a saturated solution of toluidine blue, and analyzed using a Nikon Eclipse E200 microscope (Melville, NY).

RESULTS

***In silico* analysis of the putative PHA synthases.** The *B. japonicum* USDA 110 genome contains five ORFs encoding putative PHA synthases. All of them seem to be monocistronic and are at different locations in the genome, and none of them has neighboring genes related to PHA metabolism. To further characterize these ORFs, we constructed a tree based on a multiple-sequence alignment using a maximum likelihood method with 1,000 bootstraps (see Fig. S2 in the supplemental material). While PhaC1 and PhaC3 belonged to class I PHA synthases, PhaC4 grouped with class IV PHA synthases, PhaC5 grouped with class III/IV PHA synthases, and PhaC2 grouped with five unclassified sequences (four from the betaproteobacteria and one from the alphaproteobacteria), which indicated a considerable diversity of these ORFs within the *B. japonicum* USDA 110 genome. Interestingly, PhaC1 and PhaC2 were closely related to the only two PhaC paralogs of *Rhodopseudomonas palustris*.

The *phaC1*, *phaC2*, and *phaC3* genes encode proteins of 600, 613, and 572 amino acids, respectively, while the *phaC4* and *phaC5* genes encode proteins of 360 and 371 amino acids, respectively. A multiple-sequence alignment of all these ORFs indicated that the C-terminal portions are conserved, while the N-terminal portions in PhaC1, PhaC2, and PhaC3 are longer than those in PhaC4 or PhaC5 (see Fig. S3 in the supplemental material). The C-terminal portions of the five ORFs contain a catalytic triad (C339, D491, and H519 in PhaC1), a tryptophan essential for dimerization (W437 in PhaC1), and the conserved lipase box GXCXG (33). In particular, in PhaC2 the lipase box is GXCLG, which is conserved with the other five sequences of this unclassified PHA synthase group.

PhaC1, PhaC2, and PhaC3 may indeed have two domains. Using fold assignment techniques, we found a carboxy-terminal domain starting at residue 220 of PhaC1 that probably adopts a fold similar to that of a lipase from *Sulfolobus solfataricus* (Protein Data Bank [PDB] accession number PDB 2rau; FFAS03 score, −41.2; HHpred E value, $1.4\ 10^{-27}$; both the FFAS03 score and HHpred E value are statistically significant). With *ab initio* fold prediction, we obtained tertiary models with two domains, mainly based on the structure of epoxide hydrolase 2 from *Homo sapiens* (PDB accession number 1s8o; Z score, −6.33). The N-terminal domain has an alpha-helix fold, and the C-terminal domain is similar to that obtained with fold assignment techniques (see Fig. S4 in the supplemental material). Since the main function of the N-terminal domain might be dimer stabilization (34), dimerization of PhaC4 and PhaC5, which have only one domain with a fold assignment similar to that of the C-terminal domain of the other three putative PHA synthases, might be disfavored. It was reported that full functional activity of class III and IV PHA syn-
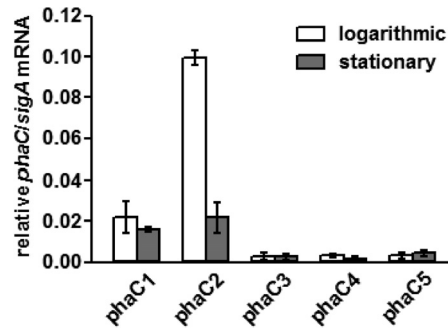
FIG 1 Quantification of *phaC* paralog mRNAs in free-living *B. japonicum* USDA 110 cells at logarithmic and stationary phases. mRNAs were obtained at logarithmic phase (6 days old) or stationary phase (18 days old). Relative mRNA levels are normalized as the ratio of *phaC* mRNA levels to constitutive *sigA* mRNA levels. Results are representative of three different experiments. Each bar represents the mean ± SEM.

thases requires an additional polypeptide that noncovalently associates with the catalytic subunit in place of the missing N-terminal domain (33). However, homologs to such a polypeptide, named PhaE or PhaR, were not found in the *B. japonicum* USDA 110 genome.

Expression and functionality of *phaC* genes. The expression of *phaC1* and *phaC2* has been documented previously (9). To extend this knowledge to the other *phaC* paralogs, we performed real-time PCR (qRT-PCR) of the five *phaC* genes with *B. japonicum* USDA 110 cultures of two ages: 6 days of growth (OD_{500} = 0.3, corresponding to logarithmic phase) and 18 days of growth (OD_{500} = 1.5, corresponding to stationary phase). As shown in Fig. 1, only *phaC1* and *phaC2* were expressed at a significant rate in relation to the level of expression of *sigA*, used as a constitutive control. In particular, *phaC2* had a high expression level in young cultures. Nevertheless, it was reported that small amounts of PHA synthase are sufficient for PHA synthesis and accumulation, while 5-fold increases in intracellular PHA synthase did not lead to a considerable increase of PHA in *Pseudomonas oleovorans* (35). Therefore, to better evaluate the significance of these different *phaC* expression levels, we obtained single mutants with mutations disrupting the catalytic triad in each of these genes and measured their PHA production. In agreement with the very low level of *phaC3*, *phaC4*, and *phaC5* expression, mutation of these genes

did not cause significant differences of PHA contents with respect to that of the wild type (not shown). Meanwhile, the *phaC1* mutant was severely impaired for PHA production, and on the contrary, the *phaC2* mutant produced different PHA levels than the wild type (see below).

In view of these results, we performed a more detailed analysis of the *phaC1* and *phaC2* mutant strains in both the free-living and symbiotic states to assess the effects of different PHA accumulation levels on growth, survival, nodulation, and plant growth promotion. In order to unambiguously refer to the specific deletions analyzed here, these strains were named LP 4360 and LP 6073 (the numbers make reference to the ORFs altered). We also included in the following analysis a double mutant, the Δ*phaC1* Δ*phaC2* mutant, which was named LP 6060.

Growth of *phaC* mutants. The growth kinetics of LP 4360 (Δ*phaC1*) and LP 6073 (Δ*phaC2*) were analyzed in detail by recording the total biomass as the OD_{500} measurement and the number of viable cells as the number of CFU in YMA (Fig. 2). At early stationary phase (6 to 10 days), LP 4360 exhibited higher viable cell counts but a lower OD_{500} than the wild-type strain and LP 6073 (Fig. 2B). Accordingly, at the same growth state, the LP 4360 and LP 6060 cells were shorter (1.79 ± 0.38 μm and 1.54 ± 0.47 μm, respectively) than the wild-type cells (3.26 ± 0.88 μm). At late stationary phase, LP 4360 and LP 6060 had lower viable cell counts than the wild type but similar OD_{500} measurements (Fig. 2A), which might indicate a higher proportion of dead cells in those cultures. The Δ*phaC2* strain LP 6073 behaved similarly to the wild type during the growth period examined, except in late stationary phase, when it had more viable cells than the wild type.

PHA accumulation in *phaC1* or *phaC2* mutants in the free-living state. The wild-type strain *B. japonicum* USDA 110 as well as the Δ*phaC2* mutant LP 6073 produced typical refringent PHA granules at late stationary phase (18 days), as observed by transmission electron microscopy (Fig. 3). Interestingly, the granules produced by LP 6073 were larger than those produced by the wild type. In contrast, neither the Δ*phaC1* LP 4360 single mutant nor the Δ*phaC1* Δ*phaC2* LP 6060 double mutant produced PHA granules.

To better analyze the PHA production by USDA 110 and LP 6073, we quantified their PHA content throughout their growth period in Götz minimal medium (Fig. 4A). In USDA 110, PHA accumulated with culture age, as has been previously observed
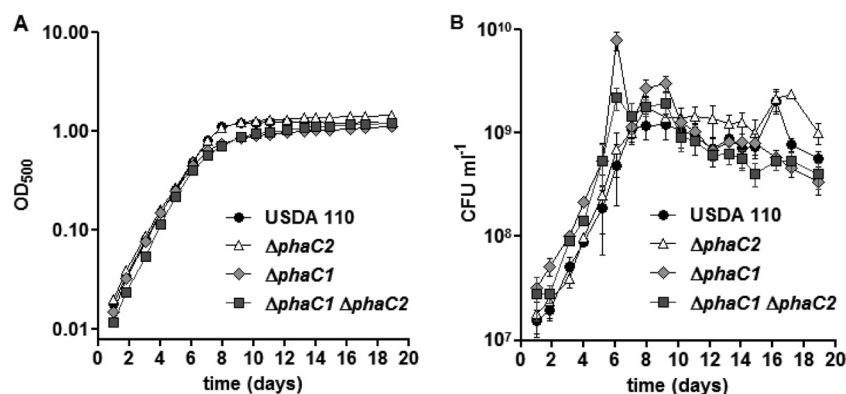

FIG 2 Growth kinetics of wild-type *B. japonicum* USDA 110 and Δ*phaC1*, Δ*phaC2*, and Δ*phaC1* Δ*phaC2* mutants. Growth was evaluated as the OD_{500} measurement (A) or the number of CFU ml^{-1} ± SD (B). When errors bars are absent, they are smaller than the symbol.
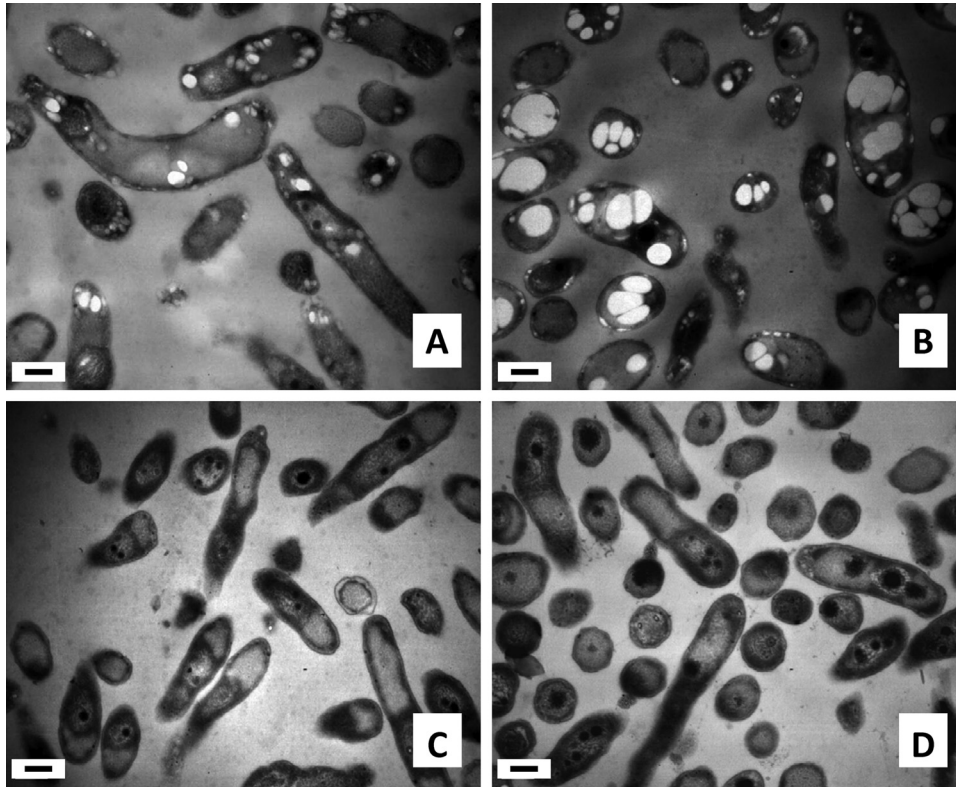
FIG 3 Electron micrographs of free-living (18-day-old) *B. japonicum* cells showing refringent PHA granules. Dark spots resembling polyphosphate granules. (A) USDA 110; (B) Δ*phaC2* mutant; (C) Δ*phaC1* mutant; (D) Δ*phaC1* Δ*phaC2* mutant. Bars, 0.5 μm.

([16](#)). Meanwhile, LP 6073 (Δ*phaC2*) produced 50% less PHA than the wild-type strain in logarithmic phase (6 days), but later, PHA production sharply increased, reaching 228% more PHA than that in the wild type at the beginning of stationary phase (9 days) and then stabilizing to 35% more PHA than that in the wild type in old cultures (41 days), in agreement with the larger PHA granules observed in this strain under the microscope. The strains carrying the *phaC1* deletion (LP 4360 and LP 6060) produced a very low level of chrotonic acid during PHA determination, in agreement with their lack of PHA granules.

The results presented above suggested that only *phaC1* is required for PHA synthesis in *B. japonicum* USDA 110. To corroborate this finding, we complemented each mutant with *phaC1* or *phaC2* in logarithmic cultures (6 days old). As expected, the absence of PHA in *phaC1* deletion mutants LP 4360 and LP 6060 could be reversed by *trans* complementation with *phaC1* but not with *phaC2* (Fig. 4B), although PHA levels in the complemented cells were higher than those in the wild type. Regarding the *phaC2* deletion mutant LP 6073, which at this growth state produced less PHA than the wild type, *trans* complementation with *phaC2* restored the intracellular PHA amounts to wild-type levels. However, the complementation of LP 6073 with *phaC1* significantly increased the PHA content, as in the *phaC1*-complemented Δ*phaC1* mutants, suggesting that PhaC1 overproduction from the plasmid led to increases in PHA synthesis in the three mutants. We were unable to perform these complementation experiments at stationary phase due to the poor growth for a prolonged time in the presence of tetracycline.

In *Rhodospirillum rubrum*, which has three *phaC* paralogs, de-

letion of *phaC1* and *phaC3* leads to an increase of PhaC2 ([36](#)). To assess whether deletion of *phaC2* in LP 6073 caused a differential expression of other *phaC* paralogs in *B. japonicum* that could explain the higher accumulation of PHA observed by us (Fig. 3 and 4A), we performed qRT-PCR of all *phaC* genes in LP 6073. As shown in Fig. 5, the expression of *phaC3* in logarithmic phase was significantly higher than that in the wild type (Fig. 1). In parallel with this change in expression, PHA levels were restored to the wild-type levels in the LP 7337 Δ*phaC2* Δ*phaC3* double mutant (Fig. 4C), suggesting that PhaC3 is active in the LP 6073 mutant background.

Survival of *B. japonicum* USDA 110 and Δ*phaC1* and Δ*phaC2* strains. To determine whether PHA levels affect cell survival, we grew the wild type and Δ*phaC1* or Δ*phaC2* mutant strain to late stationary phase (20 days) in Götz minimal medium, transferred the growth to carbon- and nitrogen-free Fåhraeus mineral solution ([37](#)), and continued the incubation for an additional 60 days at the same temperature and agitation. Similar to the wild type, all the *B. japonicum phaC* mutants analyzed showed a small but statistically nonsignificant increase in CFU numbers in this carbon- and nitrogen-free solution (see Fig. S5 in the supplemental material). This increase might simply reflect the completion of cell cycles initiated in the previous growth in culture medium using raw materials obtained by recycling of cellular components. Nevertheless, this result indicates that *B. japonicum* does not depend on PHA storage for its long-term survival.

PHA accumulation in Δ*phaC1* or Δ*phaC2* mutant bacteroids. Macroscopically, the nodules produced by all of the mutant strains appeared to be normal, and the central region of
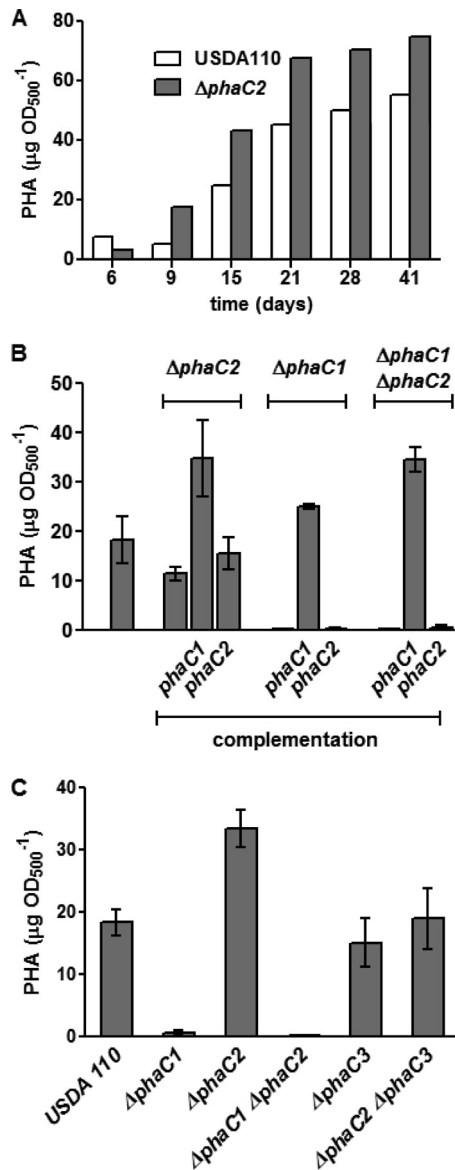
FIG 4 PHA levels in free-living cells of wild-type *B. japonicum* USDA 110 and *phaC* mutant cultures. PHA quantities (μg/ml) are normalized in relation to culture biomass (OD_{500}). (A) PHA content of the wild type and the Δ*phaC2* mutant harvested at different time points along the growth period; (B) average PHA content (±SD) of the wild type and Δ*phaC2*, Δ*phaC1*, and Δ*phaC1* Δ*phaC2* mutants at logarithmic growth phase (6 days old) and the same mutant strains complemented in *trans* with pFAJ1708 carrying either *phaC1* or *phaC2* wild-type genes; (C) PHA levels of wild type and different *phaC* single and double mutants at stationary growth phase (15 days old).
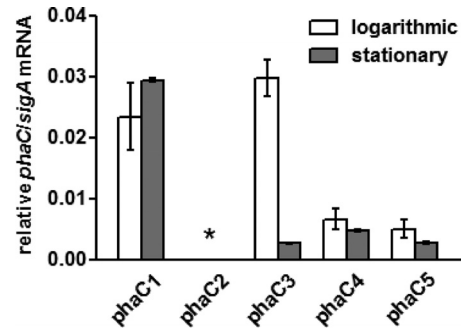

FIG 5 Quantification of *phaC* paralog mRNAs in logarithmic and stationary phases of free-living *B. japonicum* LP 6073 (Δ*phaC2*) cells. mRNAs were obtained at logarithmic phase (6 days old) or stationary phase (18 days old). Relative mRNA levels are normalized as the ratio of *phaC* mRNA levels to constitutive *sigA* mRNA levels. *, deleted *phaC2* gene. Results are representative of three different experiments. Each bar represents the mean ± SEM.

mination of PHA levels from crushed nodules obtained at the V6 stage corroborated these observations (Fig. 7).

Accumulation of PHA enhances competitiveness for nodulation. PHA is an energy reserve which can be mobilized during infection and nodule invasion. Therefore, strains that produce PHA may have an advantage in competition for nodulation against strains that lack this polymer. To see whether the accumulation of PHA is related to the competitiveness of *B. japonicum* for soybean nodulation, we coinoculated late-log-phase cultures of the wild-type USDA 110 strain with each mutant strain on soybean plants. In addition, similar competition experiments were performed between the mutants.

Mutant strains LP 4360 (Δ*phaC1*) and LP 6060 (Δ*phaC1* Δ*phaC2*), which cannot synthesize PHA, were less competitive for nodule occupancy than the wild-type strain (Table 2). In contrast, mutant strain LP 6073 (Δ*phaC2*), which synthesizes more PHA, was more competitive with both the wild-type strain and the PHA-defective mutants (Table 2), indicating a correlation between PHA accumulation and competitiveness.

Dry mass accumulation in soybean plants inoculated with different PHA mutants. Because the role of PHA in nitrogen fixation in different rhizobia is controversial (38–40) and there are no data available for *B. japonicum*, we decided to investigate whether the lack of PHA or excess PHA affects the accumulation of dry mass in soybean plants cultured in an N-free plant nutrient solution.

Soybeans were inoculated with USDA 110, LP 4360, LP 6060, or LP 6073 and grown for 70 days. The plants were then harvested, and the shoot dry mass, nodule dry mass, and nodule number per plant were recorded. As shown in Table S2 in the supplemental material, all of these parameters were statistically significantly similar among the plants that had been inoculated with the different bacterial strains.

DISCUSSION

The five *phaC* paralogs of *B. japonicum* USDA 110 were studied by bioinformatics analysis and site-directed mutagenesis. The bioinformatics analysis suggested that the encoded PHA synthases have a common C-terminal catalytic domain but only three of them have the N-terminal domain that might be involved in PhaC dimer stabilization. These paralogs seem to have evolved from

these nodules was uniformly infected with bacteria (data not shown).

The pattern of PHA granule formation in the nodule bacteroids of soybean plants at the V5 phenological stage was similar to the pattern in free-living cells that was described above. The USDA 110 and LP 6073 (Δ*phaC2*) bacteroids produced PHA granules (Fig. 6A and B), although those produced by LP 6073 were larger and more abundant, while the LP 4360 (Δ*phaC1*) and LP 6060 (Δ*phaC1* Δ*phaC2*) nodule bacteroids were devoid of PHA granules (Fig. 6C and D). Furthermore, the analytical deter-
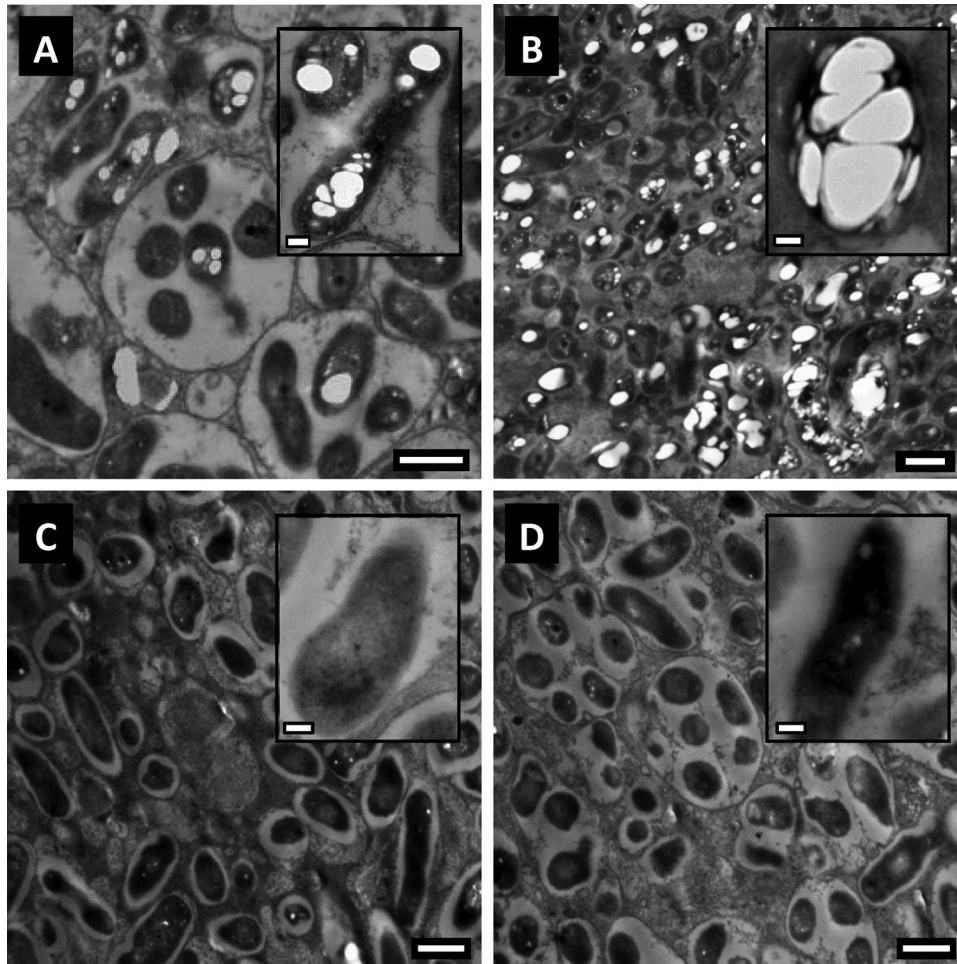
FIG 6 Electron micrographs of soybean nodules inoculated with USDA 110 (A), the $\Delta phaC2$ mutant (B), the $\Delta phaC1$ mutant (C), and the $\Delta phaC1 \Delta phaC2$ mutant (D). In panels A and B, typical refringent PHA granules inside bacteroids can be observed; these granules are absent in panels C and D. Bars, 1 μm; bars in insets, 0.2 μm.

different lineages, as PhaC1 belongs to class I PHA synthases and is similar to other rhizobial PHA synthases, PhaC2 is related to non-rhizobial unclassified PHA synthases from the betaproteobacteria, and PhaC3 belongs to well-known class I PHA synthases but is unrelated to rhizobial PHA synthases, while PhaC4 and PhaC5

belong to class III and IV PHA synthases that generally occur in taxa belonging to the *Firmicutes*, *Cyanobacteriaceae*, and *Gamma-proteobacteria*. To our knowledge, this is the most remarkable PHA synthase diversity observed within a single bacterial genome. Despite this diversity, only *phaC1* and *phaC2* were significantly expressed in wild-type strain USDA 110, and in agreement with
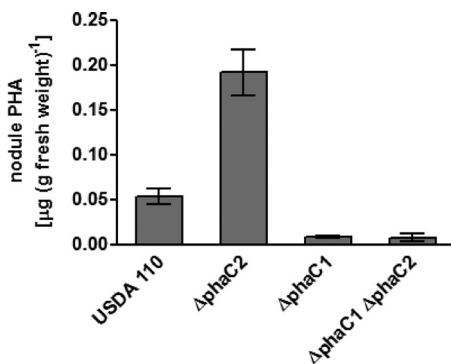

FIG 7 Average PHA content (±SD) from soybean nodules obtained from plants at the V6 stage that were inoculated with *B. japonicum* USDA 110 or the $\Delta phaC2$, $\Delta phaC1$, or $\Delta phaC1 \Delta phaC2$ mutant derivatives.

TABLE 2 Competition for nodulation of *Bradyrhizobium japonicum* USDA 110 and derived *phaC* mutants coinoculated at the indicated proportions on soybean[a]

Competitor strains	Inoculum mixture (%)	Nodule occupancy (%)	No. of plants tested	No. of nodules analyzed
USDA 110 vs $\Delta phaC2$ mutant	51:49	19:81[b]	23	311
USDA 110 vs $\Delta phaC1$ mutant	54:46	87:13[b]	16	212
USDA 110 vs $\Delta phaC1 \Delta phaC2$ mutant	47:53	85:15[b]	15	178
$\Delta phaC1$ mutant vs $\Delta phaC2$ mutant	55:45	15:85[b]	10	139

[a] The inoculum was approximately 1×10^6 CFU ml^{-1} of each competitor strain.
[b] Significantly different from the null hypothesis (45%:55%), with *P* being <0.01.

this expression profile, single mutations in these genes provoked alterations in PHA accumulation, while single mutations in *phaC3*, *phaC4*, or *phaC5* did not produce appreciable changes in bacterial PHA contents.

Several other bacterial species have two or more *phaC* genes in their genomes. Among the best-studied species harboring multiple *phaC* genes, the most related to *B. japonicum* is *Ralstonia eutropha* H16. This strain has two *phaC* genes: *phaC1* encodes an active class I PHA synthase that is more closely related to *B. japonicum* PhaC3 than to *B. japonicum* PhaC1, and *phaC2* encodes an unclassified PHA synthase that belongs to the same group as *B. japonicum* PhaC2, has no catalytic activity *in vitro*, and is unable to complement a *phaC1* mutation in *R. eutropha*. In addition, *R. eutropha* H16 *phaC2* is not transcribed (41). In *B. japonicum*, the ΔphaC1 mutant was unable to synthesize PHA, while the ΔphaC2 mutant accumulated more PHA than the wild-type strain, both in liquid culture at stationary phase and in mature soybean nodules. Hence, similar to *R. eutropha* PhaC2, *B. japonicum* PhaC2 may be a catalytically inactive PHA synthase or a negative regulator of PHA biosynthesis, as has been suggested for *Rhodospirillum rubrum* PhaC1 (33). In *B. japonicum* USDA 110, *phaC2* was transcribed at similar or even higher levels than *phaC1*, suggesting that this paralog may play a role in the PHA metabolism of this species.

The active PHA synthase of *R. eutropha* is homodimeric (42), while in *R. rubrum*, homo- and heterodimers are both active *in vitro* (33). Therefore, it might be speculated that in wild-type *B. japonicum* free-living and bacteroid cells, catalytically active PhaC1$_2$ and catalytically inactive PhaC2$_2$ homodimers, as well as a PhaC1-PhaC2 heterodimer that exhibits intermediate catalytic activity, are formed. Therefore, the combined amounts of PhaC1 and PhaC2 might determine the global PHA synthase activity in the cell, and as suggested by our complementation experiments, a relative increase of PhaC1 might lead to higher PHA accumulation. This hypothesis could explain why the *phaC1* mutant was unable to produce PHA and the *phaC2* mutant produced more polymer than the wild-type strain at stationary phase. In addition, at the onset of PHA synthesis, PhaC is soluble in the cytoplasm, but as the PHA granule grows, PhaC molecules bind to the surface of the granule, where they express their full catalytic activity (42). Since the PHA granules tend to be spherical, their surface/volume ratio diminishes as the PHA granules grow. Therefore, if the early increase in *phaC2* transcript levels observed in this study results in a later increase in PhaC2 protein levels, this paralog would soon occupy the limited PhaC sites on the granule surface, thus disturbing the access of PhaC1, which might lead to a diminished biosynthetic activity, or it may preclude the access of a PHA depolymerase enzyme. The interplay between PhaC1 and PhaC2 might be relevant in nodules, where *phaC2* expression is stimulated 6-fold by FixK2 (a transcription factor enhancer that is stimulated by low O$_2$ levels) (10). Surprisingly, *phaC3*, which was poorly expressed in the wild type, was upregulated at logarithmic growth phase in the ΔphaC2 mutant. Such a differential accumulation of a PhaC paralog as a consequence of mutation in another *phaC* paralog was already observed recently in *R. rubrum* (36). We have no explanation for this emergent property, but mutation in *phaC3* in the ΔphaC2 background restored the PHA levels to those of the wild type, indicating that in this background PhaC3 was in part responsible for PHA synthesis, in addition to PhaC1. Nevertheless, the results obtained with the ΔphaC1 ΔphaC2 double mutant as well as in the complementation experiments clearly indicate

that PhaC1 is required for PHA synthesis, a function that cannot be fulfilled by PhaC3 alone. Further *in vitro* experiments with purified PhaC1, PhaC2, and PhaC3 are required to shed light on the functionality and association of these three proteins.

The competitiveness of the *phaC* mutants for nodulation was correlated with their PHA levels, in agreement with previous reports of lower competitiveness of PHA-deficient *E. meliloti* mutants in alfalfa (38, 40). The invasion of plant tissues toward the nodule requires the cells to traverse a stressful environment (43–46), and it was observed that *B. japonicum* cells that are deficient in α-ketoglutarate dehydrogenase produce nodule primordia that abort at higher rates. This observation suggests that energy must be efficiently produced by the rhizobia to complete root infection (47). Because PHA is a carbon- and energy-reserve polymer, higher levels of this polymer may help the cells to complete infection and nodule invasion in this metabolically unfavorable situation (5), thus explaining the observed correlation between PHA levels and nodulation competitiveness.

In contrast to the effects on competition for nodulation, PHA levels had no effect on the production of shoot or nodule biomass. These results are similar to those that have been obtained in other determinate nodule symbiotic systems. Soybean plants that have been nodulated by *B. japonicum* USDA 110 isocitrate dehydrogenase mutants, which have increased PHA levels in their nodules, produce similar shoot dry weight and acetylene reduction activity as those that have been nodulated by the wild type (48). Moreover, *Phaseolus vulgaris* plants that have been inoculated with a *phaC*-defective strain of *Rhizobium leguminosarum* 8401 carrying the pRL2JI (*Rhizobium phaseoli*) pSym plasmid produce similar shoot dry weight as plants that have been inoculated with the wild-type strain (49). In contrast, other studies reported increased nitrogen fixation activity and biomass production in *P. vulgaris* plants that had been inoculated with a *phaC*-defective mutant of *Rhizobium etli* CFN42 (39). These authors suggested that PHA synthesis may compete with nitrogenase for the reducing power in the nodule. If this hypothesis is true, these apparently contradictory results may be explained because, unlike *R. etli* CFN42, *B. japonicum* USDA 110 possesses the hydrogenase uptake (*hup*) system, which recycles the hydrogen produced in the nitrogenase reaction, thus supplying extra reducing power (50, 51). Although the *hup* system has been detected in several *R. leguminosarum* strains, it is unknown whether the 8401 strain possesses it.

REFERENCES

1. **Doyle JJ.** 1998. Phylogenetic perspectives on nodulation: evolving views of plants and symbiotic bacteria. Trends Plant Sci. **3**:473–478.
2. **Patriarca EJ, Tatè R, Ferraioli S, Iaccarino M.** 2004. Organogenesis of legume root nodules. Int. Rev. Cytol. **234**:201–262.

3. **Oono R, Schmitt I, Sprent JI, Denison RF.** 2010. Multiple evolutionary origins of legume traits leading to extreme rhizobial differentiation. New Phytol. **187:**508–520.

4. **Verlinden RAJ, Hill DJ, Kenward MA, Williams CD, Radecka I.** 2007. Bacterial synthesis of biodegradable polyhydroxyalkanoates. J. Appl. Microbiol. **102:**1437–1449.

5. **Trainer MA, Charles TC.** 2006. The role of PHB metabolism in the symbiosis of rhizobia with legumes. Appl. Microbiol. Biotechnol. **71:**377–386.

6. **Ratcliff WC, Kadam SV, Denison RF.** 2008. Poly-3-hydroxybutyrate (PHB) supports survival and reproduction in starving rhizobia. FEMS Microbiol. Ecol. **65:**391–399.

7. **Kaneko T, Nakamura Y, Sato S, Minamisawa K, Uchiumi T, Sasamoto S, Watanabe A, Idesawa K, Iriguchi M, Kawashima K, Kohara M, Matsumoto M, Shimpo S, Tsuruoka H, Wada T, Yamada M, Tabata S.** 2002. Complete genomic sequence of nitrogen-fixing symbiotic bacterium *Bradyrhizobium japonicum* USDA 110. DNA Res. **9:**189–197.

8. **Sarma AD, Emerich DW.** 2005. Global protein expression pattern of *Bradyrhizobium japonicum* bacteroids: a prelude to functional proteomics. Proteomics **5:**4170–4184.

9. **Pessi G, Ahrens CH, Rehrauer H, Lindemann A, Hauser F, Fischer H-M, Hennecke H.** 2007. Genome-wide transcript analysis of *Bradyrhizobium japonicum* bacteroids in soybean root nodules. Mol. Plant Microbe Interact. **20:**1353–1363.

10. **Mesa S, Hauser F, Friberg M, Malaguti E, Fischer HM, Hennecke H.** 2008. Comprehensive assessment of the regulons controlled by the FixLJ-FixK2-FixK1 cascade in *Bradyrhizobium japonicum*. J. Bacteriol. **190:**6568–6579.

11. **Reutimann L, Mesa S, Hennecke H.** 2010. Autoregulation of $fixK_2$ gene expression in *Bradyrhizobium japonicum*. Mol. Genet. Genomics **284:**25–32.

12. **Franck WL, Chang W-S, Qiu J, Sugawara M, Sadowsky MJ, Smith SA, Stacey G.** 2008. Whole-genome transcriptional profiling of *Bradyrhizobium japonicum* during chemoautotrophic growth. J. Bacteriol. **190:**6697–6705.

13. **Delmotte N, Ahrens CH, Knief C, Qeli E, Koch M, Fischer H-M, Vorholt JA, Hennecke H, Pessi G.** 2010. An integrated proteomics and transcriptomics reference data set provides new insights into the *Bradyrhizobium japonicum* bacteroid metabolism in soybean root nodules. Proteomics **10:**1–10.

14. **Koch M, Delmotte N, Rehrauer H, Vorholt JA, Pessi G, Hennecke H.** 2010. Rhizobial adaptation to hosts, a new facet in the legume root-nodule symbiosis. Mol. Plant Microbe Interact. **23:**784–790.

15. **Aneja P, Dai M, Lacorre DA, Pillon B, Charles TC.** 2004. Heterologous complementation of the exopolysaccharide synthesis and carbon utilization phenotypes of *Sinorhizobium meliloti* Rm1021 polyhydroxyalkanoate synthesis mutants. FEMS Microbiol. Lett. **239:**277–283.

16. **Quelas JI, López-García SL, Casabuono A, Althabegoiti MJ, Mongiardini EJ, Pérez-Giménez J, Couto A, Lodeiro AR.** 2006. Effects of N-starvation and C-source on *Bradyrhizobium japonicum* exopolysaccharide production and composition, and bacterial infectivity to soybean roots. Arch. Microbiol. **186:**119–128.

17. **Vincent JM.** 1970. A manual for the practical study of the root nodule bacteria. IBP handbook no. 15. Blackwell Scientific Publications, Oxford, United Kingdom.

18. **Regensburger B, Hennecke H.** 1983. RNA polymerase from *Rhizobium japonicum*. Arch. Microbiol. **135:**103–109.

19. **Sambrook J, Russell D.** 2001. Molecular cloning: a laboratory manual, 3rd ed. Cold Spring Harbor Laboratory Press, Cold Spring Harbor, NY.

20. **Quelas JI, Mongiardini EJ, Casabuono A, López-García SL, Althabegoiti MJ, Covelli JM, Pérez-Giménez J, Couto A, Lodeiro AR.** 2010. Lack of galactose or galacturonic acid in *Bradyrhizobium japonicum* USDA 110 exopolysaccharide leads to different symbiotic responses in soybean. Mol. Plant Microbe Interact. **23:**1592–1604.

21. **Dombrecht B, Vanderleyden J, Michiels J.** 2001. Stable RK2-derived cloning vectors for the analysis of gene expression and gene function in Gram-negative bacteria. Mol. Plant Microbe Interact. **14:**426–430.

22. **Notredame C, Higgins DG, Heringa J.** 2000. T-Coffee: a novel method for fast and accurate multiple sequence alignment. J. Mol. Biol. **302:**205–217.

23. **Guindon S, Dufayard JF, Lefort V, Anisimova M, Hordijk W, Gascuel O.** 2010. New algorithms and methods to estimate maximum-likelihood phylogenies: assessing the performance of PhyML 3.0. Syst. Biol. **59:**307–321.

24. **Tamura K, Peterson D, Peterson N, Stecher G, Nei M, Kumar S.** 2011. MEGA5: molecular evolutionary genetics analysis using maximum likelihood, evolutionary distance, and maximum parsimony methods. Mol. Biol. Evol. **28:**2731–2739.

25. **Jaroszewski L, Rychlewski L, Li Z, Li W, Godzik A.** 2005. FFAS03: a server for profile-profile sequence alignments. Nucleic Acids Res. **33**(Web Server issue):W284–W288.

26. **Söding J, Remmert M, Biegert A, Lupas AN.** 2006. HHsenser: exhaustive transitive profile search using HMM-HMM comparison. Nucleic Acids Res. **34**(Web Server issueW374–W378.

27. **Roy A, Kucukural A, Zhang Y.** 2010. I-TASSER: a unified platform for automated protein structure and function prediction. Nat. Protoc. **5:**725–738.

28. **Wiederstein M, Sippl MJ.** 2007. ProSA-web: interactive web service for the recognition of errors in three-dimensional structures of proteins. Nucleic Acids Res. **35**(Web Server issueW407–W410.

29. **Hauser F, Lindemann A, Vuilleumier S, Patrignani A, Schlapbach R, Fischer HM, Hennecke H.** 2006. Design and validation of a partial-genome microarray for transcriptional profiling of the *Bradyrhizobium japonicum* symbiotic gene region. Mol. Genet. Genomics **275:**55–67.

30. **Law JH, Slepecky RA.** 1961. Assay of poly-beta-hydroxybutyric acid. J. Bacteriol. **82:**33–36.

31. **Althabegoiti MJ, Covelli JM, Pérez-Giménez J, Quelas JI, Mongiardini EJ, López MF, López-García SL, Lodeiro AR.** 2011. Analysis of the role of the two flagella of *Bradyrhizobium japonicum* in competition for nodulation of soybean. FEMS Microbiol. Lett. **319:**133–139.

32. **Schneider CA, Rasband WS, Eliceiri KW.** 2012. NIH Image to ImageJ: 25 years of image analysis. Nat. Methods **9:**671–675.

33. **Rehm BHA.** 2003. Polyester synthases: natural catalysts for plastics. Biochem. J. **376:**15–33.

34. **Argiriadi MA, Morisseau C, Hammock BD, Christianson DW.** 1999. Detoxification of environmental mutagens and carcinogens: structure, mechanism, and evolution of liver epoxide hydrolase. Proc. Natl. Acad. Sci. U. S. A. **96:**10637–10642.

35. **Kraak MN, Smits TH, Kessler B, Witholt B.** 1997. Polymerase C1 levels and poly(R-3-hydroxyalkanoate) synthesis in wild-type and recombinant *Pseudomonas* strains. J. Bacteriol. **179:**4985–4991.

36. **Jin H, Nikolau BJ.** 2012. Role of genetic redundancy in polyhydroxyalkanoate (PHA) polymerases in PHA biosynthesis in *Rhodospirillum rubrum*. J. Bacteriol. **194:**5522–5529.

37. **Fåhraeus G.** 1957. The infection of clover root hairs by nodule bacteria studied by a simple glass slide technique. J. Gen. Microbiol. **16:**374–381.

38. **Aneja P, Zachertowska A, Charles TC.** 2005. Comparison of the symbiotic and competition phenotypes of *Sinorhizobium meliloti* PHB synthesis and degradation pathway mutants. Can. J. Microbiol. **51:**599–604.

39. **Cevallos M, Encarnación AS, Leija A, Mora Y, Mora J.** 1996. Genetic and physiological characterization of a *Rhizobium etli* mutant strain unable to synthesize poly-beta-hydroxybutyrate. J. Bacteriol. **178:**1646–1654.

40. **Povolo S, Tombolini R, Morea A, Anderson AJ, Casella S, Nuti MP.** 1994. Isolation and characterization of mutants of *Rhizobium meliloti* unable to synthesize poly-β-hydroxybutyrate (PHB). Can. J. Microbiol. **40:**823–829.

41. **Peplinski K, Ehrenreich A, Döring C, Bömeke M, Reinecke F, Hutmacher C, Steinbüchel A.** 2010. Genome-wide transcriptome analyses of the 'Knallgas' bacterium *Ralstonia eutropha* H16 with regard to polyhydroxyalkanoate metabolism. Microbiology **156:**2136–2152.

42. **Jendrossek D.** 2009. Polyhydroxyalkanoate granules are complex subcellular organelles (carbonosomes). J. Bacteriol. **191:**3195–3202.

43. **Brechenmacher L, Lei Z, Libault M, Findley S, Sugawara M, Sadowsky MJ, Sumner LW, Stacey G.** 2010. Soybean metabolites regulated in root hairs in response to the symbiotic bacterium *Bradyrhizobium japonicum*. Plant Physiol. **153:**1808–1822.

44. **Jones KM, Kobayashi H, Davies BW, Taga ME, Walker GC.** 2007. How rhizobial symbionts invade plants: the *Sinorhizobium-Medicago* model. Nat. Rev. Microbiol. **5:**619–633.

45. **Miyahara A, Richens J, Starker C, Morieri G, Smith L, Long S, Downie JA, Oldroyd GE.** 2010. Conservation in function of a SCAR/WAVE component during infection thread and root hair growth in *Medicago truncatula*. Mol. Plant Microbe Interact. **23:**1553–1562.

46. **Vinuesa P, Neumann-Silkow F, Pacios-Bras C, Spaink HP, Martínez-Romero E, Werner D.** 2003. Genetic analysis of a pH-regulated operon

from *Rhizobium tropici* CIAT899 involved in acid tolerance and nodulation competitiveness. Mol. Plant Microbe Interact. **16**:159–168.

47. **Green LS, Emerich DW.** 1999. Light microscopy of early stages in the symbiosis of soybean with a delayed-nodulation mutant of *Bradyrhizobium japonicum.* J. Exp. Bot. **50**:1577–1585.

48. **Shah R, Emerich AD.** 2006. Isocitrate dehydrogenase of *Bradyrhizobium japonicum* is not required for symbiotic nitrogen fixation with soybean. J. Bacteriol. **188**:7600–7608.

49. **Lodwig EM, Leonard M, Marroqui S, Wheeler TR, Findlay K, Downie JA, Poole PS.** 2005. Role of polyhydroxybutyrate and glycogen as carbon storage compounds in pea and bean bacteroids. Mol. Plant Microbe Interact. **18**:67–74.

50. **Leyva A, Palacios JM, Murillo J, Ruiz-Argüeso T.** 1990. Genetic organization of the hydrogen uptake (*hup*) cluster from *Rhizobium leguminosarum.* J. Bacteriol. **172**:1647–1655.

51. **Schubert KR, Jennings NT, Evans HJ.** 1978. Hydrogen reactions of nodulated leguminous plants. II. Effects on dry matter accumulation and nitrogen fixation. Plant Physiol. **61**:398–401.

52. **Figurski DH, Helinski DR.** 1979. Replication of an origin-containing derivative of plasmid RK2 dependent on a plasmid function provided in trans. Proc. Natl. Acad. Sci. U. S. A. **76**:1648–1652.

53. **Schäfer A, Tauch A, Jäger W, Kalinowski J, Thierbach G, Pühler A.** 1994. Small mobilizable multi-purpose cloning vectors derived from the *Escherichia coli* plasmids pK18 and pK19: selection of defined deletions in the chromosome of *Corynebacterium glutamicum.* Gene **145**: 69–73.

54. **Kirchner O, Tauch A.** 2003. Tools for genetic engineering in the amino acid-producing bacterium *Corynebacterium glutamicum.* J. Biotechnol. **104**:287–299.

55. **Kovach ME, Elzer PH, Hill DS, Robertson GT, Farris MA, Roop RM, Peterson KM.** 1995. Four new derivatives of the broad-host range cloning vector pBBR1MCS, carrying different antibiotic-resistance cassettes. Gene **166**:175–176.

56. **Prentki P, Krisch HM.** 1984. *In vivo* insertional mutagenesis with a selectable DNA fragment. Gene **29**:303–313.

57. **Vieira J, Messing J.** 1982. The pUC plasmids, an M13mp7-derived system for insertion mutagenesis and sequencing with synthetic universal primers. Gene **19**:259–268.

58. **Simon R, Priefer U, Pühler A.** 1983. Vector plasmids for in vivo and in vitro manipulations of Gram negative bacteria, p 98–106. *In* Pühler A (ed), Molecular genetics of the bacteria-plant interaction. Springer, Berlin, Germany.